forests

MDPI

Article

Tree-Ring Chronologies from the Upper Treeline in the Russian Altai Mountains Reveal Strong and Stable Summer Temperature Signals

Alexander V. Kirdyanov [1,2,3,*], Alberto Arzac [3], Alina A. Kirdyanova [4], Tito Arosio [1], Dmitriy V. Ovchinnikov [2], Dmitry A. Ganyushkin [4], Paul N. Katjutin [4,5], Vladimir S. Myglan [3], Andrey N. Nazarov [3], Igor Y. Slyusarenko [6], Tatiana Bebchuk [1] and Ulf Büntgen [1,7,8]

1 Department of Geography, University of Cambridge, Cambridge CB2 3EN, UK; ta530@cam.ac.uk (T.A.); tb649@cam.ac.uk (T.B.); ub223@cam.ac.uk (U.B.)
2 Sukachev Institute of Forest SB RAS, Federal Research Center 'Krasnoyarsk Science Center SB RAS', Akademgorodok, Krasnoyarsk 660036, Russia; dovch@mail.ru
3 Institute of Ecology and Geography, Siberian Federal University, 79 Svobodnii, Krasnoyarsk 660041, Russia; aarzac@gmail.com (A.A.); v.myglan@gmail.com (V.S.M.); nazar_69@mail.ru (A.N.N.)
4 Institute of Earth Sciences, St. Petersburg State University, St. Petersburg 199034, Russia; akird2002@mail.ru (A.A.K.); ganushkinspbgu@mail.ru (D.A.G.); paurussia@binran.ru (P.N.K.)
5 Botanical Institute of RAS, ul. Professor Popov 2, St. Petersburg 197022, Russia
6 Institute of Archaeology and Ethnography SB RAS, Pr. Akademika Lavrentieva 17, Novosibirsk 630090, Russia; slig1963@yandex.ru
7 Department of Geography, Masaryk University, 61137 Brno, Czech Republic
8 Global Change Research Centre, 61300 Brno, Czech Republic
* Correspondence: ak2118@cam.ac.uk

Abstract: Radial tree growth at high-elevation and high-latitude sites is predominantly controlled by changes in summer temperature. This relationship is, however, expected to weaken under projected global warming, which questions the reliability of tree-ring chronologies for climate reconstructions. Here, we examined the growth–climate response patterns of five tree-ring width (TRW) and maximum latewood density (MXD) chronologies of larch (*Larix sibirica*) from upper-treeline ecotones in the Altai Mountains, which is a key region for developing millennial-long dendroclimatic records in inner Eurasia. The TRW and MXD chronologies exhibited significant year-to-year coherency within and between the two parameters ($p < 0.001$). While TRW is mostly influenced by temperature changes during the first half of the growing season from June to July ($r = 0.66$), MXD is most strongly correlated with May–August temperatures ($r = 0.73$). All seasonal temperature signals are statistically significant at the 99% confidence level, temporally stable back to 1940 CE, the period with reliable instrumental measurements, and spatially representative for a vast area of inner Eurasia between northeastern Kazakhstan in the west, northern Mongolia in the east, southern Russia in the north and northwestern China in the south. Our findings demonstrate the paleoclimatic potential of TRW and especially MXD chronologies and reject any sign of the ´divergence problem´ at these high-elevation, mid-latitude larch sites.

Keywords: climate reconstruction potential; dendroclimatology; divergence problem (DP); global warming; spatiotemporal homogeneity

Citation: Kirdyanov, A.V.; Arzac, A.; Kirdyanova, A.A.; Arosio, T.; Ovchinnikov, D.V.; Ganyushkin, D.A.; Katjutin, P.N.; Myglan, V.S.; Nazarov, A.N.; Slyusarenko, I.Y.; et al. Tree-Ring Chronologies from the Upper Treeline in the Russian Altai Mountains Reveal Strong and Stable Summer Temperature Signals. *Forests* **2024**, *15*, 1402. https://doi.org/10.3390/f15081402

Academic Editor: Steve Chhin

Received: 2 July 2024
Revised: 29 July 2024
Accepted: 3 August 2024
Published: 10 August 2024

1. Introduction

Tree growth in most of the high-elevation and high-latitude regions in Eurasia is currently temperature-sensitive and predominantly controlled by summer temperature variability [1]. Tree-ring data from such regions are considered a valuable climate proxy and are widely used in reconstructions of local to global temperatures [2]. However, the

dependence of tree growth on temperature is expected to weaken under projected global warming and even decouple from temperature during the 21st century [3].

The loss of sensitivity of tree growth in ecosystems presumably limited by temperature to rising summer temperatures in high- or low-frequency domains or both, the so-called 'divergence problem' (DP) [4], was first reported for white spruce (*Picea glauca*) in Alaska [5]. The study demonstrated weakened signals of the tree-ring width and maximum latewood density at high-latitude and high-elevation sites in response to increasing temperatures since the late 1970s. Lately, the DP has been described for a variety of tree species in different regions, mostly in high-latitude and high-elevation ecosystems (see [4] for a review). Briffa et al. [6] and Wilson et al. [7] provided evidence of the DP as a widespread phenomenon in circum-polar high-latitude forests. The DP was also found in several high-elevation forests in lower latitudes [8–10]. However, some recent studies have shown that the DP is not observed in all temperature-limited sites, implying that the DP is a spatially heterogeneous phenomenon [2,11–13]. A better understanding of the scale and regionality of the DP is required as this phenomenon may affect the ability of tree-ring data to serve as a proxy for temperature during past warm periods [2]. Special attention has to be paid to regions with high paleo-dendroclimatic potential, like the Altai Mountains [14,15].

The Altai Mountains are one of the largest mountain ranges in Asia, which extends between 47–53° N and 84–92° E and lies in the cross-border region extending into Russia in the north, China in the south, Kazakhstan in the south-west, and Mongolia in the south-east. Altai serves as a crucial climatic boundary, where North Atlantic climatic systems from the west interact with Pacific climatic systems from the east. This interaction has led to recent temperature increases in both North and South Altai [16]. The area is an origin of long-living trees [17] and a source of relict wood, which is used to develop multi-millennia-long tree-ring width (TRW) chronologies [14,18–20] and shorter, but extremely valuable, chronologies of other tree-ring parameters, including the maximum latewood density (MXD), tree-ring stable isotope composition, cell structure, and blue intensity (BI) [21–23]. These data provide information not only on forest dynamics in the region [24–27] but also allow an understanding of tree growth's dependence on the climate and serve as proxies for different climate variables, such as temperature [15,19,28,29], precipitation [30,31], droughts [32,33], air relative humidity [34], and frost events [35].

Tree-ring-based reconstructions from the Altai Mountains and neighboring mountain ridges serve as a basis for understanding climate variability over a vast region in Central Asia [15,36]. These data can be matched with climate dynamics reconstructed from ice cores [37], elemental contents [38], pollen data from lake sediments [39,40], pollen data from soil profiles and geomorphological data [41], and lipids from peat cores [42]. In this context, the further development and updating of the existing tree-ring network in the Altai Mountains and understanding the recent changes in tree rings' response to the climate under current warming are urgent. Special attention has to be paid to TRW and MXD measurements from the upper treeline because these parameters are usually closely connected to summer temperature changes and may, consequently, be prone to the DP.

Here, we explored the radial growth and climate sensitivity of five upper treeline larch sites across Central Altai. We analyzed the temporal stability and spatial extent of the climatic response of recently developed tree-ring width and maximum latewood density chronologies to test their exposure to the 'divergence problem' and assess their reconstruction potential. We hypothesized that tree growth in the study region is directly affected by climate warming, and tree-ring parameters retain their sensitivity to temperature changes.

2. Materials and Methods

Wood samples were collected at upper treeline sites in the Altai Mountains (Figure 1). According to the instrumental records from the high-elevation meteorological station Kara-Tyurek (50°02′ N, 86°27′ E; WMO 36442; 1940–2022), the climate in the study area is characterized as extremely continental, with low annual mean temperatures of −5.4 °C. The warmest and coldest months are July and January, with monthly temperatures of 7.1 °C

and −16.4 °C, respectively. The annual precipitation totals are around 620 mm, of which 46% fall during summer months (from June to August).

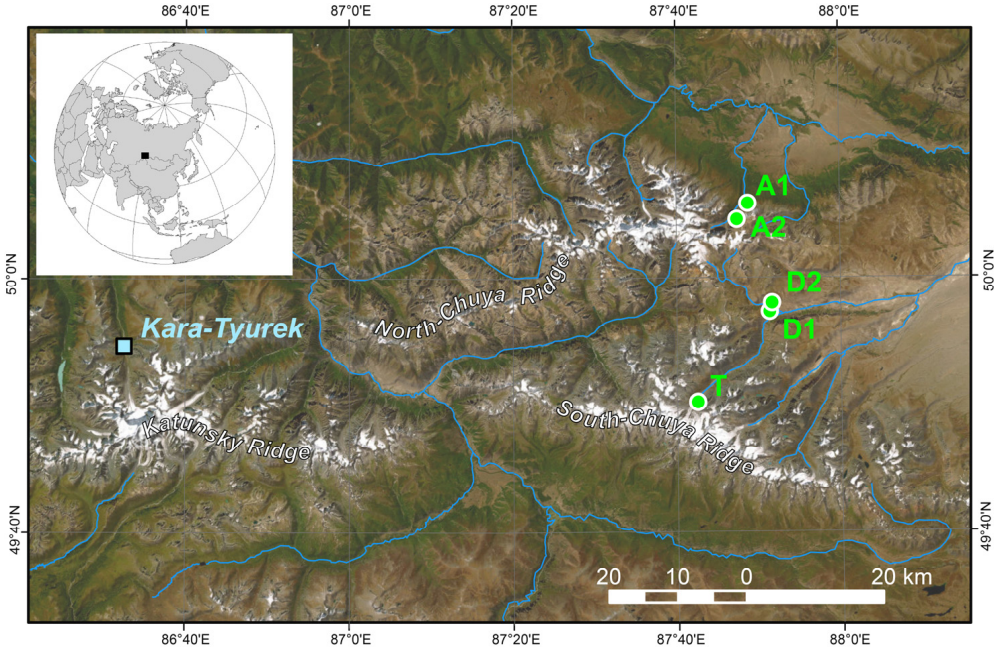

Figure 1. Location of the tree-ring sampling sites (light-green circles) and the meteorological station (light-blue square).

The annual and summer (June–August) temperature means were relatively stable till the beginning of the 1980s (Figure 2a). Since 1983, temperatures have been increasing by 0.38 and 1.33 °C/decade annually and in summer, respectively ($p < 0.001$). The annual and summer precipitation totals have not shown statistically significant changes ($p > 0.05$) (Figure 2b).

Siberian larch (*Larix sibirica* Ledeb.), which was shown to be sensitive to summer temperature variability [14,15,22,23], is one of the dominant tree species at the upper treeline in the study region. During several field campaigns between 2007 and 2023, we sampled five different stands in the upper treeline ecotone in three valleys in Central Altai associated with the glaciers Ak-Tru (sites A1 and A2), Djelo (D1 and D2), and Taldura (T) (Figures 1 and S1–S4; Tables 1 and S1). We collected wood from healthy dominant and co-dominant living larch trees at elevations from 2100–2150 m a.s.l. at site A2 to 2400–2500 at site T. At all the sites, except A2, larch was the only tree species. Although we aimed to core the old-growth trees, the stand at the highest site T was formed of larch trees of <100 years old because it has developed in an area recently covered by a glacier [43]. A minimum of 16 living trees were cored, with at least two cores per tree, of which one core was used for further TRW and MXD measurements. At three sites, A2, D2, and T, the TRW was measured at an accuracy of 0.01 mm using a LINTAB measurement device and the TSAPWin 4.68c software (RINNTECH e.K., Heidelberg, Germany). For the cores from sites A1 and D1, we measured the TRW and MXD using a DENDRO-2003 X-ray microdensitometer (WALESCH Electronic GmbH, Effretikon, Switzerland) according to [44]. All the series were visually cross-dated and statistically checked for missing rings and dating errors using the program COFECHA 6.06 [45].

The individual TRW and MXD series were standardized to remove non-climatic, tree geometry, and age-related trends [46]. Due to the different average ages of the trees at the sites, the individual TRW and MXD series were standardized with an age-dependent cubic spline (ARSTAN software version v49, https://www.geog.cam.ac.uk/research/projects/dendrosoftware/, last accessed on 25 June 2024). In addition, prior to growth trend removal, adaptive power transformation (PT; [47]) was applied to the MXD series. The

bi-weight robust means of the individual measurement series were calculated to produce dimensionless index chronologies. The standard versions of the chronologies were chosen in further analyses to trace the trends in the climatic data.

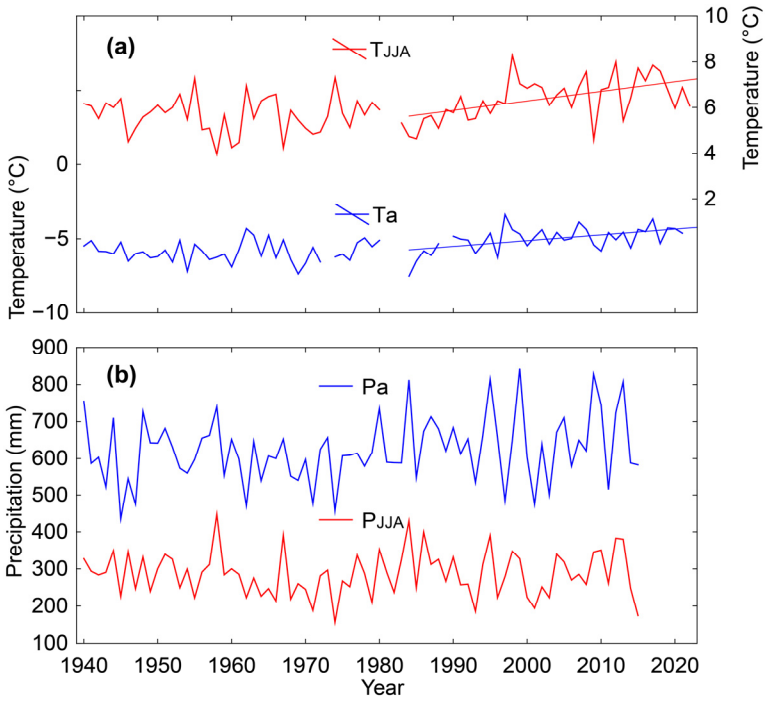

Figure 2. Summer (red) and annual mean (blue) temperatures (**a**) and precipitation (**b**) recorded at the high-elevation Kara-Tyurek meteorological station near the tree sites. Lines indicate statistically significant ($p < 0.05$) trends over time since 1984.

Table 1. Statistics of tree-ring width (TRW) and maximum latewood density (MXD) local chronologies (MSL = mean segment length (mean ± SD = mean TRW or MXD value ± standard deviation); CS = coefficient of sensitivity; Rbar = inter-series correlation; EPS = expressed population signal).

Site	Elevation, m a.s.l.	Tree-Ring Parameter	N of Series	Period CE	MSL	Mean ± SD	Mean CS	Mean Rbar	Mean EPS
A1	2200–2300	TRW	18	1653–2014	262	0.67 ± 0.32 mm	0.202	0.472	0.916
A2	2100–2150	TRW	20	1554–2021	269	0.79 ± 0.35 mm	0.225	0.508	0.915
D1	2200–2300	TRW	23	1478–2006	325	0.42 ± 0.22 mm	0.271	0.503	0.925
D2	2360–2400	TRW	16	1715–2021	198	0.62 ± 0.30 mm	0.310	0.520	0.899
T	2400–2500	TRW	20	1936–2022	63	1.17 ± 0.44 mm	0.234	0.456	0.925
A1	2200–2300	MXD	18	1653–2014	262	0.86 ± 0.10 g/cm^3	0.07	0.526	0.934
D1	2200–2300	MXD	23	1478–2006	325	0.86 ± 0.10 g/cm^3	0.08	0.531	0.934

In total, we developed five local (site) TRW and two MXD chronologies (Table 1). The lengths of the TRW chronologies varied from 87 (site T) to 529 (D1) years, with the lowest and highest mean segment length (MSL) for the same sites, respectively. The average growth rate was generally lower in older trees. The TRW chronologies were sensitive to an environmental signal (coefficient of sensitivity > 0.200), which synchronized the radial growth of individual trees and explained the high inter-series correlation (Rbar > 0.456). The multi-century MXD chronologies were also characterized by a high Rbar but a much lower sensitivity compared with the TRW. The expressed population signal (EPS), which measures how well chronologies built on a limited number of samples represent a theoretically infinite population, was higher than the commonly accepted threshold of 0.85 [48] for all TRW and MXD chronologies. The replication of 16 to 23 series and the high Rbar and EPS values confirmed the suitability of the TRW and MXD index chronologies for

dendroclimatic analysis during the period with the available temperature and precipitation instrumental records.

For further analyses, we also used regional chronologies, which were calculated as the averages of the local index chronologies in ARSTAN. The regional TRW chronology was built from the five local TRW index chronologies, and the two local MXD index chronologies were used to build the regional MXD chronology. This procedure allowed us to equalize the weights of the data from sites with different local conditions, sample replications, and tree ages.

To evaluate the climate sensitivity of the TRW and MXD records, Pearson's correlation coefficients were calculated against the monthly temperature means and precipitation totals from the nearest meteorological station Kara-Tyurek from the previous year September–September of the current year. The June–July (JJ), summer (JJA), and May–August (MJJA) temperatures, as well as the total precipitation during summer, were used to assess the seasonal climatic influences. To estimate the temporal stability of the relations between the regional tree-ring chronologies and climate records, we used the running correlations calculated for a 25-year window with a 1-year step with growing seasonal temperature means. The spatial correlations between the regional TRW and MXD chronologies and gridded seasonal temperature means (CRU TS4.07, [49]) were calculated with the KNMI Climate Explorer (https://climexp.knmi.nl/start.cgi, last accessed on 25 June 2024) for the period with the available instrumental temperature records at the nearest high-elevation station Kara-Tyurek from 1940.

3. Results

The local TRW index chronologies demonstrated high synchronicity in the radial growth indices in different sites (Table 2; Figure 3). High statistically significant correlations ($p < 0.000001$) of up to $r = 0.79$ (N = 362) were observed between the four longer chronologies A1, A2, D1, and D2. For the shortest chronology T, the correlations were lower but statistically significant at $p < 0.002$. The correlation between the two available MXD index chronologies was higher than that for TRW, at $r = 0.62$ and 0.49 (N = 354), respectively. There were also notable correlations between the TRW and MXD records from the same sites, which varied from $r = 0.50$ (N = 362) for A1 to $r = 0.71$ (N = 529) for site D1.

Table 2. Correlation coefficients and number of cases (N) between the local index chronologies.

Site	A2	D1	D2	T
A1	**0.79** N = 362	**0.49** N = 354	**0.48** N = 300	0.36 N = 79
A2		**0.61** N = 453	**0.52** N = 307	0.50 N = 86
D1			**0.63** N = 292	0.50 N = 71
D2				0.33 N = 86

Note: Correlation coefficients are significant at $p < 0.002$, and values significant at $p < 0.000001$ are marked in **bold**.

The regional TRW and MXD index chronologies demonstrated a common pattern of high- and medium-frequency variability (Figure 3). Remarkably low index values in both records were observed around the year 1700 CE and during the first decades of the 19th century. Later, the indices were characterized by a generally increasing trend till the last decade of the 20th century. Interestingly, both the TRW and MXD indices generally stabilized or even decreased in the 21st century. The correlation coefficient between the regional chronologies was 0.63 (N = 537; $p < 0.000001$), which increased to 0.73 for the records smoothed with a 30-year cubic spline.

The monthly climate response analysis showed that the TRW of larch in the upper treeline was mostly dependent on temperature from May to July (Figure 4a). The highest correlations were found for the local A1 ($r = 0.58$), A2 ($r = 0.55$), and T ($r = 0.54$) and regional

(r = 0.60) index chronologies with the June temperature means. The correlations with May temperatures were generally lower and statistically significant ($p < 0.05$) only for A2, D1, and the regional chronologies. July temperatures were important for secondary tree growth at all the sites, except D2. The correlations of the TRW standard chronologies with the seasonal mean temperatures were generally higher than those with the monthly means, especially for JJ (up to r = 0.66 with a regional chronology; $p < 0.01$).

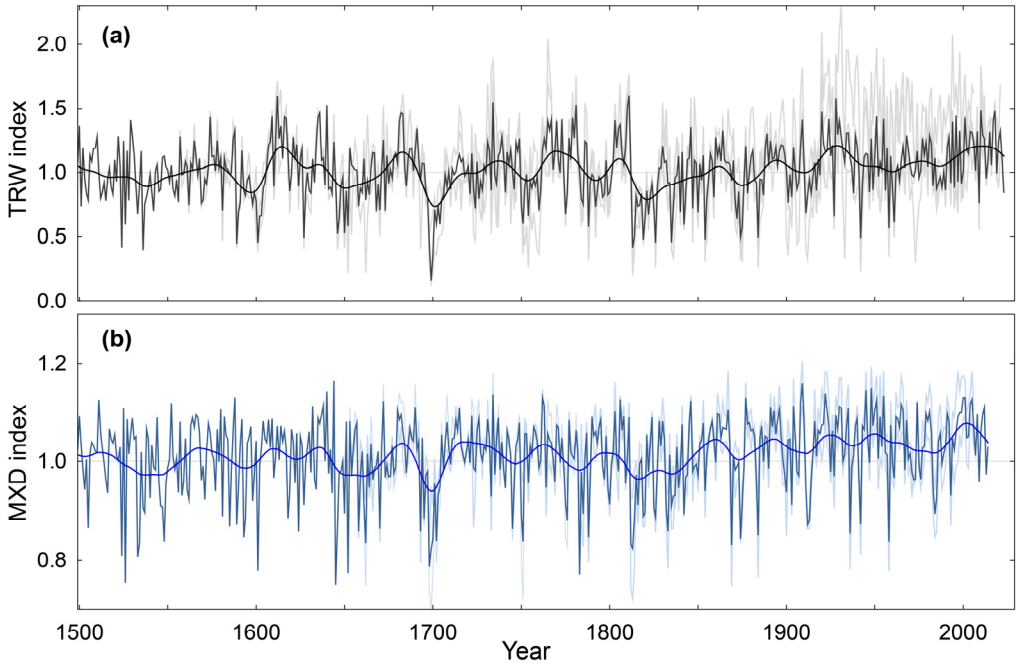

Figure 3. Regional tree-ring width (TRW) (**a**) and maximum latewood density (MXD) (**b**) chronologies with local index chronologies shown in light color. The chronologies were smoothed with a 30-year cubic spline.

The MXD was influenced by temperature variability over a longer interval of the growing season than the TRW (Figure 4b). The correlations of the MXD index chronologies with the monthly temperature means were statistically significant ($p < 0.05$) from May to August and showed the lowest and the highest values in August (up to r = 0.30 for D1) and July (up to r = 0.61 for D1), respectively. For the seasonal temperature means, the correlations further increased and reached the highest values with the temperature of the extended May–August period (r = 0.69, 0.74, and 0.73 for A1, D1, and the regional chronologies, respectively; $p < 0.01$).

The correlations of the tree-ring parameters with the monthly precipitation totals were lower than those with the temperature (Table S2). Statistically significant ($p < 0.05$) negative values were observed for the TRW mainly in the June instrumental record for sites A2 (r = −0.23), D2 (−0.26), and T (−0.28) and the regional chronology (−0.24). The MXD negatively correlated with the July precipitation totals at A1 (r = −0.35) and A2 (−0.45) and regionally (−0.41).

The 25-year window running correlations between the TRW regional chronology and seasonal temperature means showed that the dependence of radial growth on temperature was positive and mostly statistically significant at $p < 0.05$ over the period from 1940 (Figure 5a). All three sequences of running correlation coefficients were characterized by slightly decreasing trends toward the present. Generally higher correlations were observed over time for JJ temperatures (mean r = 0.63), which reached $r > 0.7$ during the first part of the analyzed period and, later, fell to around 0.55 ($p < 0.01$). The correlation of the MXD with the seasonal temperature means was stronger than that for TRW, with the correlation coefficients often being higher than 0.8 (Figure 5b). The dependence of the MXD

on temperature was stable over time, and the mean correlations were slightly higher for MJJA (r = 0.78) than for JJA (0.77) and JJ (0.76).

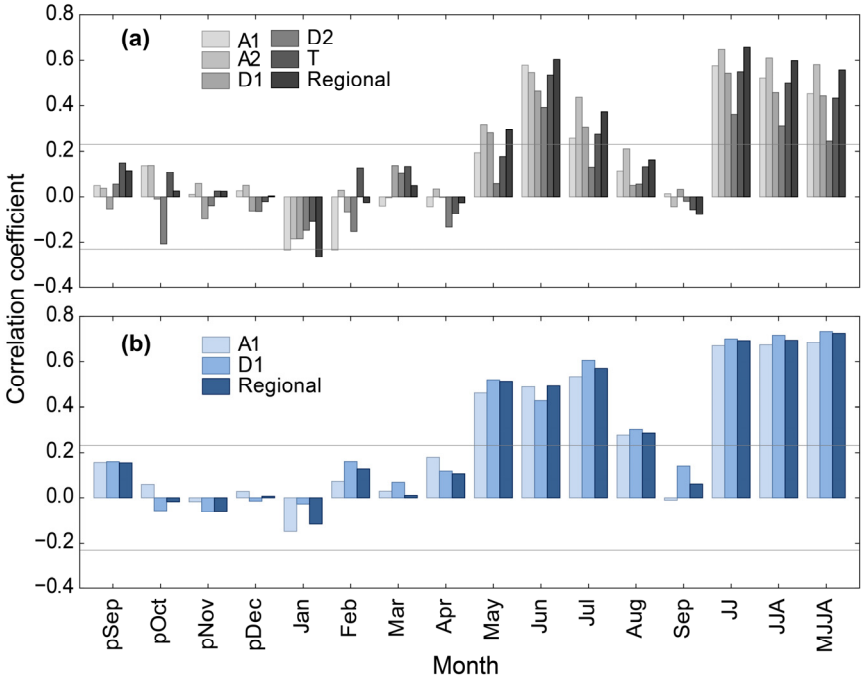

Figure 4. Correlation coefficients between standard tree-ring width (**a**) and maximum latewood density (**b**) local and regional chronologies and monthly temperature means from the previous year September–September of ring formation and seasonal temperature means for June–July (JJ), summer (JJA), and from May to August (MJJA). Grey horizontal lines indicate the significance level $p < 0.05$.

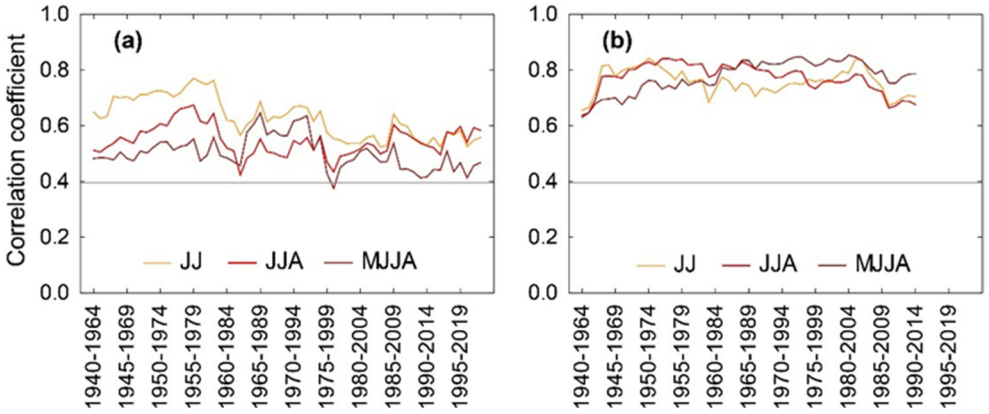

Figure 5. Twenty-five-year window running correlations between the regional tree-ring width (**a**) and maximum latewood density (**b**) index chronologies and seasonal temperature means of June–July (JJ), summer (JJA), and May–August (MJJA). Grey horizontal lines indicate the significance level $p < 0.05$.

Both the TRW and MXD regional chronologies well captured the inter-annual and multi-decadal changes in the JJ and MJJA instrumental temperature records, respectively (Figure 6). Following the tendencies in the temperature changes, the regional tree-ring chronologies were characterized by a slightly decreasing trend in the 21st century, which followed the increase from the 1980s and relatively stable decadal temperatures before that. The high correlations obtained between the annually resolved tree-ring and climate records (see Figure 4) further increased to 0.97 (N = 83) between the TRW and JJ and 0.85 (N = 75) between the MXD and MJJA temperatures for the records smoothed with a 30-year spline (Figure 6).

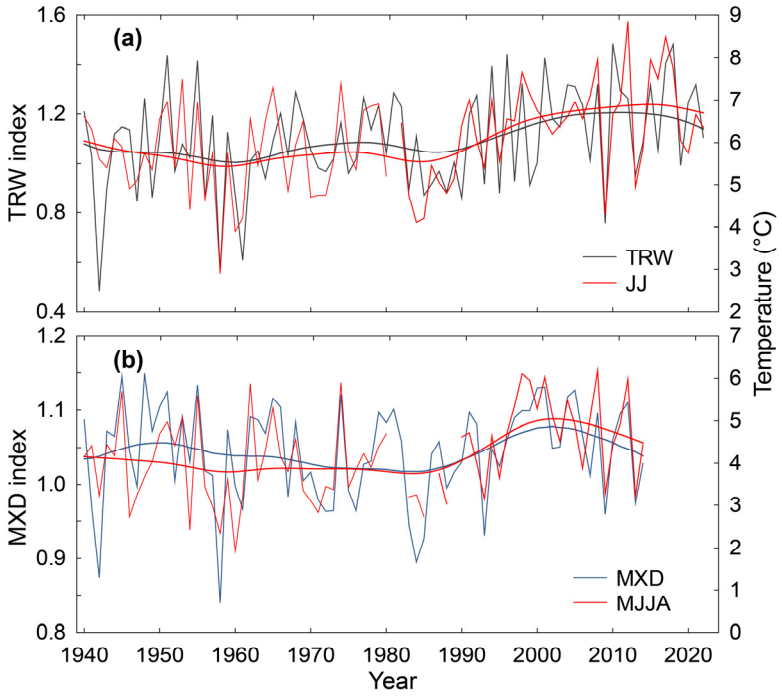

Figure 6. Tree-ring width (TRW) scaled against June–July (JJ) temperature means (**a**) and maximum latewood density (MXD) versus May–August (MJJA) temperature means (**b**). The chronologies were smoothed with a 30-year cubic spline.

The spatial temperature signature of the MXD regional chronology (Figure 7b) was larger than that of the TRW (Figure 7a). However, the high field correlations of the tree-ring records with the gridded summer temperature means covered a substantial fraction of southern Siberia and northern Inner Asia.

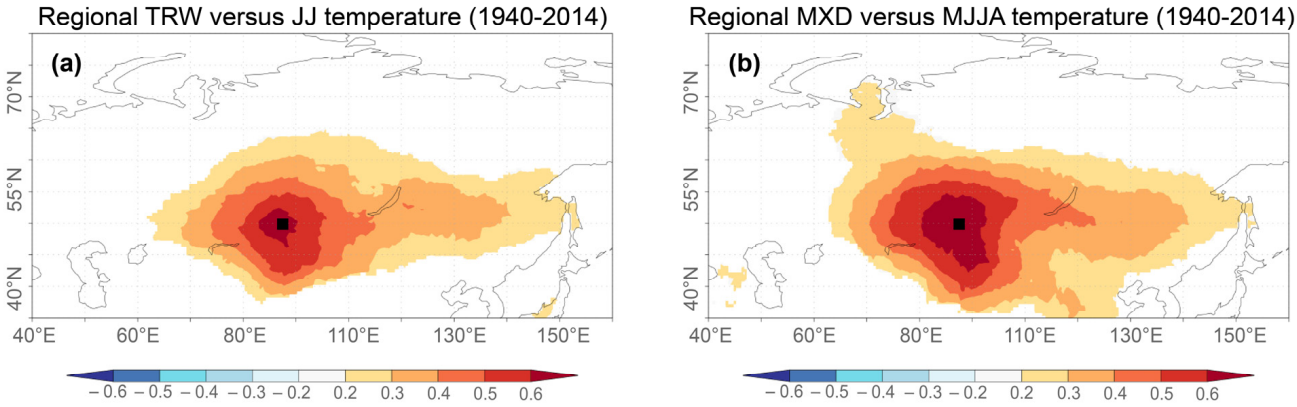

Figure 7. Correlation fields of tree-ring width (TRW) (**a**) and maximum latewood density (MXD) (**b**) regional chronologies against gridded June–July (JJ) and May–August (MJJA) averaged temperature means (TS4.07, [49]) for the period of 1940–2014. Black rectangles indicate the study region. Built with KNMI Climate Explorer (https://climexp.knmi.nl/start.cgi, last accessed on 25 June 2024).

4. Discussion

Our results show that larch trees at the upper treeline in the central Altai Mountains exhibit highly coherent growth in different environments. The altitudinal range of 350 m of the study sites located from 2100 to 2450 m a.s.l. corresponds to an approximately 2 °C difference in the mean annual temperature between the habitats [50]. Such a temperature difference may lead to considerable site-specific changes in the intra- and inter-annual variability of tree seasonal activity in larch [51,52]. Local conditions, including slope,

aspect, stand density, ground vegetation, exposure to wind, permafrost conditions, etc., can further significantly modulate tree radial growth dynamics [53–57]. However, despite the differences in local conditions, the TRW and MXD were highly synchronized within and between our study sites, indicating that there is a common climate factor strongly limiting tree growth within the region.

Previous studies in Altai and neighboring mountain regions have indicated summer temperature as the main factor that defines tree radial growth at the upper treeline [15,29,57–59], and our results confirm these earlier findings (Figure 3). Temperature signatures were earlier found not only in the TRW and MXD but also in other tree-ring parameters, including the latewood cell wall thickness, stable isotope composition of tree-ring cellulose, and BI [21,22,60]. However, the MXD typically has greater accuracy in capturing meteorological information [12,61–63], and it is usually considered the highest-quality tree-ring proxy variable for temperature reconstructions [64,65]. Cell structure data can sometimes perform better than the MXD in representing growing seasonal temperatures [22,66]; however, the process of wood anatomy measurements is even more labor- and time-consuming than that for MXD. In this context, the approaches that rely on a binary (black–white) representation of anatomical structures on the surfaces of tree-ring samples and combine the advances of the BI, wood anatomy, and MXD techniques are promising [61,67,68].

In this study, we showed that the MXD is highly correlated with temperature variables and accumulates climate information over a longer period of the growing season (May–August) compared with the TRW (June–July). This phenomenon is well-known in tree-ring science [44,69,70] and is explained by the physiology and phenology of tree-ring and latewood formation [23,71,72]. These findings confirm the superiority of larch MXD from the upper treeline in Altai as a proxy for growing seasonal temperatures. The wide spatial coverage of the statistically significant correlations demonstrates the ability of our tree-ring records to capture temperature signals over a vast area of inner Eurasia, which includes north-eastern Kazakhstan in the west, north-western Mongolia in the east, southern Siberia (Russia) in the north, and north-eastern China in the south.

We found that both tree-ring parameters and especially MXD demonstrated a highly temporally stable sensitivity to the growing seasonal temperature. Moreover, the chronologies followed the recent warming and temperature stabilization in the last few years (Figure 6). These findings testify to the absence of the "divergence problem" in the study area. Although the DP is a region- and site-specific phenomenon [11,13], we assume that the upper treeline in the Altai Mountains is less prone to the weakening of the growth–temperature coupling because the DP is usually less pronounced in mid-latitudes [6,73], and Altai is remote from industrial pollution sources [74]. Moreover, the summer temperature in the upper treeline at the study sites in the Altai Mountains is still low, not reaching the threshold above which the influence of temperature on tree-ring formation drastically decreases [72]. In addition, the studied high-elevation sites are located close to glaciers and are hardly accessible, receiving no direct impact from human activity.

Currently, Altai is one of the few regions in the world where (i) tree rings provide reliable information on temperature changes, (ii) old trees are growing [17], and (iii) relict wood is available. A number of millennia-long chronologies have already been produced in the region [14,19]. The current efforts of our team are directed toward the construction of continuous absolutely dated well-replicated regional TRW and MXD chronologies, which cover the past two–three millennia. In this context, our findings of the wide spatial signature and temporal stability of temperature signals in the TRW, and especially MXD, are of great importance for future paleoclimatic reconstructions. When developed, an MXD-based regional temperature reconstruction will not only provide data on the local and regional late Holocene climate but may also serve to better understand the land use and human history in the Altai Mountains [15,75,76].

5. Conclusions

The results of our study demonstrate that temperature signals in the local and regional tree-ring width and maximum latewood density chronologies of Siberian larch from the upper treeline in Central Altai are strong and temporally stable. This testifies to the absence of the 'divergence problem' in tree-ring data and indicates the high paleoclimatic potential of upper treeline larch tree-ring chronologies. Current efforts directed at developing a network of well-replicated, absolutely dated millennia-long tree-ring chronologies will be the basis for collaborative multiparameter dendroclimatology that will provide the opportunity for a better understanding of paleoclimate and human history in the Altai and surrounding regions.

Supplementary Materials: The following supporting information can be downloaded at: https://www.mdpi.com/article/10.3390/f15081402/s1. Figure S1: Site A1. Photo by D.V. Ovchinnikov; Figure S2: Site A2. Photos by A.V. Kirdyanov; Figure S3: Site D1. Photos by V.S. Myglan; Figure S4: Site T. Photos by D.A. Ganyushkin; Table S1: Site location; Table S2: Correlation coefficients between standard tree-ring width (TRW) and maximum latewood density (MXD) local and regional chronologies and monthly precipitation totals from the previous year September to September of ring formation.

Author Contributions: Conceptualization, A.V.K.; methodology, A.V.K. and U.B.; investigation, A.V.K. and T.A.; data curation A.V.K., A.A., A.A.K., D.V.O., P.N.K., V.S.M., A.N.N. and I.Y.S.; writing—original draft preparation, A.V.K. and U.B.; writing—review and editing, A.A.K., A.A., A.A.K., T.A., P.N.K., I.Y.S., T.B. and U.B.; visualization, A.V.K. and D.A.G.; funding acquisition, A.A., D.V.O., D.A.G. and U.B. All authors have read and agreed to the published version of the manuscript.

Funding: This work was supported by the projects of the Ministry of Science and Higher Education of the Russian Federation (FSRZ-2020-0014 and FSRZ-2023-0007) (which provided the equipment). The data for one of the sites were collected and analyzed under the Russian Science Foundation (project no. 22-67-00020). U.B. received funding from the Czech Science Foundation (#23-08049S; Hydro8), the ERC Advanced Grant (#882727; Monostar), and the ERC Synergy Grant (#101118880; Synergy-Plague).

Data Availability Statement: The data presented in this study are available upon request from the corresponding author.

Conflicts of Interest: The authors declare no conflicts of interest.

References

1. George, S.S. An overview of tree-ring width records across the Northern Hemisphere. *Quat. Sci. Rev.* **2014**, *95*, 132–150. [CrossRef]
2. Büntgen, U.; Allen, K.; Anchukaitis, K.; Arseneault, D.; Boucher, É.; Bräuning, A.; Chatterjee, S.; Cherubini, P.; Churakova, O.V.; Corona, C.; et al. The influence of decision-making in tree ring-based climate reconstructions. *Nat. Commun.* **2021**, *12*, 3411. [CrossRef] [PubMed]
3. Camarero, J.J.; Gazol, A.; Sánchez-Salguero, R.; Fajardo, A.; McIntire, E.J.B.; Gutiérrez, E.; Batllori, E.; Boudreau, S.; Carrer, M.; Diez, J.; et al. Global fading of the temperature-growth coupling at alpine and polar treelines. *Glob. Chang. Biol.* **2021**, *27*, 1879–1889. [CrossRef] [PubMed]
4. D'Arrigo, R.; Wilson, R.; Liepert, B.; Cherubini, P. On the 'Divergence Problem' in Northern Forests: A review of the tree-ring evidence and possible causes. *Glob. Planet. Chang.* **2008**, *60*, 289–305. [CrossRef]
5. Jacoby, G.C.; D'Arrigo, R. Tree-ring width and density evidence of climatic and potential forest change in Alaska. *Glob. Biogeochem. Cycles* **1995**, *9*, 227–234. [CrossRef]
6. Briffa, K.R.; Schweingruber, F.H.; Jones, P.D.; Osborn, T.J.; Shiyatov, S.G.; Vaganov, E.A. Reduced sensitivity of recent tree-growth to temperature at high northern latitudes. *Nature* **1998**, *391*, 678–682. [CrossRef]
7. Wilson, R.; D'Arrigo, R.D.; Buckley, B.M.; Büntgen, U.; Esper, J.; Frank, D.; Luckman, B.; Payette, S.; Vose, R.; Youngblut, D. A matter of divergence: Tracking recent warming at hemispheric scales using tree ring data. *J. Geophys. Res.* **2007**, *112*, D17103. [CrossRef]
8. Zhang, Y.; Wilmking, M.; Gou, X. Changing relationships between tree growth and climate in Northwest China. *Plant. Ecol.* **2009**, *201*, 39–50. [CrossRef]
9. Jiao, L.; Jiang, Y.; Zhang, W.T.; Wang, M.-C.; Zhang, L.-N.; Zhao, S.-D. Divergent responses to climate factors in the radial growth of *Larix sibirica* in the eastern Tianshan Mountains, northwest China. *Trees* **2015**, *29*, 1673–1686. [CrossRef]

10. Li, J.X.; Li, J.B.; Li, T.; Au, T.F. Tree growth divergence from winter temperature in the Gongga Mountains, southeastern Tibetan Plateau. *Asian Geogr.* **2020**, *37*, 1–15. [CrossRef]
11. Anchukaitis, K.J.; D'Arrigo, R.D.; Andreu-Hayles, L.; Frank, F.; Verstege, A.; Curtis, A.; Buckley, B.M.; Jacoby, G.C.; Cook, E.R. Tree-Ring-Reconstructed Summer Temperatures from Northwestern North America during the Last Nine Centuries. *J. Clim.* **2013**, *26*, 3001–3012. [CrossRef]
12. Büntgen, U.; Reinig, F.; Verstege, A.; Piermattei, A.; Kunz, M.; Krusic, P.; Slavin, P.; Štěpánek, P.; Torbenson, M.; del Castillo, E.M.; et al. Recent summer warming over the western Mediterranean region is unprecedented since medieval times. *Glob. Planet. Chang.* **2024**, *232*, 104336. [CrossRef]
13. Yin, H.; Li, M.-Y.; Huang, L. Summer mean temperature reconstruction based on tree-ring density over the past 440 years on the eastern Tibetan Plateau. *Quat. Int.* **2021**, *571*, 81–88. [CrossRef]
14. Myglan, V.S.; Oidupaa, O.C.; Vaganov, E.A. A 2367-Year Tree-Ring Chronology for the Altai–Sayan Region (Mongun-Taiga Mountain Massif). *Archaeol. Ethnol. Anthropol. Eurasia* **2012**, *40*, 76–83. [CrossRef]
15. Büntgen, U.; Myglan, V.S.; Ljungqvist, F.C.; McCormick, M.; Di Cosmo, N.; Sigl, M.; Jungclaus, J.; Wagner, S.; Krusic, P.J.; Esper, J.; et al. Cooling and societal change during the Late Antique Little Ice Age from 536 to around 660 AD. *Nat. Geosci.* **2016**, *9*, 231–236. [CrossRef]
16. Zhang, T.; Yuan, Y.; Chen, F.; Yu, C.; Zhang, R.; Qin, L.; Jiang, S. Reconstruction of hydrological changes based on tree-ring data of the Haba River, northwestern China. *J. Arid Land* **2018**, *10*, 53–67. [CrossRef]
17. Taynik, A.V.; Myglan, V.S.; Barinov, V.V.; Oidupaa, O.C.; Churakova, O.V. Ancient larch trees in the Tuva Republic, land of the oldest trees in Russia. *J. Prot. Mt. Areas Res. Manag.* **2023**, *15*, 13–19. [CrossRef]
18. Panyushkina, I.; Sljusarenko, I.; Bikov, N.; Bogdanov, E. Floating larch tree-ring chronologies from Archaeological timbers in the Russian Altai between about 800 BC and AD 800 E. *Radiocarbon* **2007**, *49*, 693–702. [CrossRef]
19. Myglan, V.S.; Oidupaa, O.C.; Kirdyanov, A.V.; Vaganov, E.A. 1929-year tree-ring chronology for the Altai-Sayan. Region (Western Tuva). *Archaeol. Ethnol. Anthropol. Eurasia* **2008**, *36*, 25–31. [CrossRef]
20. Nazarov, A.N.; Solomina, O.N.; Myglan, V.S. Absolute and relative age of moraines of the Aktru and Historical stages of glaciers of Central Altai based on lichenometry and dendrochronology. *Led i Sneg. Ice Snow* **2022**, *62*, 387–409. (In Russian)
21. Loader, N.J.; Helle, G.; Los, S.O.; Lehmkuhl, F.; Schleser, G.H. Twentieth-century summer temperature variability in the southern Altai Mountains: A carbon and oxygen isotope study of tree-rings. *Holocene* **2010**, *20*, 1149–1156. [CrossRef]
22. Sidorova, O.V.; Saurer, M.; Myglan, V.S.; Eichler, A.; Schwikowski, M.; Kirdyanov, A.V.; Bryukhanova, M.V.; Gerasimova, O.V.; Kalugin, I.A.; Daryin, A.V.; et al. A multi-proxy approach for revealing recent climatic changes in the Russian Altai. *Clim. Dyn.* **2012**, *38*, 175–188. [CrossRef]
23. Chen, F.; Yuan, Y.; Wei, W.; Fan, Z.; Zhang, T.; Shang, H.; Zhang, R.; Yu, S.; Ji, C.; Qin, L. Climatic response of ring width and maximum latewood density of *Larix sibirica* in the Altay Mountains, reveals recent warming trends. *Ann. For. Sci.* **2012**, *69*, 723–733. [CrossRef]
24. Dulamsuren, C.; Khishigjargal, M.; Leuschner, C.; Hauck, M. Response of tree-ring width to climate warming and selective logging in larch forests of the Mongolian Altai. *J. Plant Ecol.* **2014**, *7*, 24–38. [CrossRef]
25. Wu, X.; Liu, H.; He, L.; Qi, Z.; Anenkhonov, O.A.; Korolyuk, A.Y.; Yu, Y.; Guo, D. Stand-total tree-ring measurements and forest inventory documented climate-induced forest dynamics in the semi-arid Altai Mountains. *Ecol. Indic.* **2014**, *36*, 231–241. [CrossRef]
26. Cazzolla Gatti, R.; Callaghan, T.; Velichevskaya, A.; Dudko, A.; Fabbio, L.; Battipaglia, G.; Liang, J. Accelerating upward treeline shift in the Altai Mountains under last-century climate change. *Sci. Rep.* **2019**, *9*, 7678. [CrossRef] [PubMed]
27. Savchuk, D.A.; Timoshok, E.E.; Filimonova, E.O.; Nikolaeva, S.A. The dynamics of the upper forest line on the Katunsky Range (the Altai Mountains) over the last 120 years. *Russ. J. Ecol.* **2023**, *54*, 482–487. [CrossRef]
28. Adamenko, M.F. Dynamics of larch tree growth as indicator of thermical regimes of summer in the Altai Mountain. In *Regional Geographical Investigations in the Western Siberia*; Nauka: Novosibirsk, Russia, 1978; pp. 20–23. (In Russian)
29. Zhang, T.; Yuan, Y.; Hu, Y.; Wei, W.; Shang, H.; Huang, L.; Zhang, R.; Chen, F.; Yu, S.; Fan, Z.; et al. Early summer temperature changes in the southern Altai Mountains of Central Asia during the past 300 years. *Quat. Int.* **2015**, *358*, 68–76. [CrossRef]
30. Chen, F.; Yuan, Y.J.; Wei, W.S.; Zhang, T.W.; Shang, H.M.; Zhang, R.B. Precipitation reconstruction for the southern Altay Mountains (China) from tree rings of Siberian spruce, reveals recent wetting trend. *Dendrochronologia* **2014**, *32*, 266–272. [CrossRef]
31. Pang, W.; Li, Q.; Liu, Y.; Song, H.; Sun, C.; Wang, J.; Yan, Y.; Cai, Q.; Ren, M. Precipitation variations in China's Altay Mountains detected from tree rings dating back to AD 1615. *Forests* **2023**, *14*, 1496. [CrossRef]
32. Jiang, S.; Zhang, T.; Yuan, Y.; Yu, S.; Shang, H.; Zhang, R. Drought reconstruction based on tree-ring earlywood of *Picea obovata* Ledeb. for the southern Altay Mountains. *Geogr. Ann. A* **2020**, *102*, 267–286. [CrossRef]
33. Davi, N.; Jacoby, G.; Fang, K.; Li, J.; D'Arrigo, R.; Baatarbileg, N.; Robinson, D. Reconstructing drought variability for Mongolia based on a large-scale tree ring network: 1520–1993. *J. Geophys. Res.* **2010**, *115*, D22103. [CrossRef]
34. Xu, G.; Liu, X.; Qin, D.; Chen, T.; Wang, W.; Wu, G.; Sun, W.; An, W.; Zeng, X. Relative humidity reconstruction for northwestern China's Altay Mountains using tree-ring $\delta^{18}O$. *Chin. Sci. Bull.* **2014**, *59*, 190–200. [CrossRef]
35. Barinov, V.V.; Myglan, V.S.; Taynik, A.V.; Oydupaa, O.C.; Vaganov, E.A. Extreme climatic events in the Republic of Tuva according to tree-ring analysis. *Contemp. Probl. Ecol.* **2015**, *8*, 414–422. [CrossRef]

36. Oyunmunkh, B.; Weijers, S.; Loeffler, J.; Byambagerel, S.; Soninkhishig, N.; Buerkert, A.; Goenster-Jordan, S.; Simme, C. Climate variations over the southern Altai Mountains and Dzungarian Basin region, central Asia, since 1580 CE. *Int. J. Climatol.* **2019**, *39*, 4543–4558. [CrossRef]
37. Eichler, A.; Olivier, S.; Henderson, K.; Laube, A.; Beer, J.; Papina, T.; Gäggeler, H.W.; Schwikowski, M. Temperature response in the Altai region lags solar forcing. *Geophys. Res. Lett.* **2009**, *36*, L01808. [CrossRef]
38. Babich, V.V.; Daryin, A.V.; Rudaya, N.A.; Markovich, T.I. Two Millennia of Climate History for the Russian Altai: Integrated Reconstruction from Lake Sediment Data. *Russ. Geol. Geophys.* **2023**, *64*, 1217–1226. [CrossRef]
39. Blyakharchuk, T.A.; Wright, H.E.; Borodavko, P.S.; van der Knaap, W.O.; Ammann, B. Late Glacial and Holocene vegetational changes on the Ulagan high-mountain plateau, Altai Mountains, southern Siberia. *Palaeogeogr. Palaeoclimatol. Palaeoecol.* **2004**, *209*, 259–279. [CrossRef]
40. Huang, X.; Peng, W.; Rudaya, N.; Grimm, E.C.; Chen, X.; Cao, X.; Zhang, J.; Pan, X.; Liu, S.; Chen, C.; et al. Holocene vegetation and climate dynamics in the Altai Mountains and surrounding areas. *Geophys. Res. Lett.* **2018**, *45*, 6628–6636. [CrossRef]
41. Schlütz, F.; Lehmkuhl, F. Climatic change in the Russian Altai, southern Siberia, based on palynological and geomorphological results, with implications for climatic teleconnections and human history since the middle Holocene. *Veget. Hist. Archaeobot.* **2007**, *16*, 101–118. [CrossRef]
42. Rao, Z.; Guo, H.; Cao, J.; Shi, F.; Jia, G.; Li, Y.; Chen, F. Consistent long-term Holocene warming trend at different elevations in the Altai Mountains in arid central Asia. *J. Quat. Sci.* **2020**, *35*, 1036–1045. [CrossRef]
43. Ostanin, O.V.; Mikhailov, N.N. *Current Changes in High-Mountain Geosystems (Case Study of Central and South-Eastern Altai)*; Altai State University: Barnaul, Russia, 2013; 171p.
44. Schweingruber, F.H. *Tree Rings: Basics and Applications of Dendrochronology*; Kluwer Academic Publishers: Dordrecht, The Netherlands; Boston, MA, USA, 1988; 276p.
45. Holmes, R.L. Computer-assisted quality control in tree-ring datingand measurement. *Tree-Ring Bull.* **1983**, *44*, 69–75.
46. Cook, E.R.; Kairiukstis, L.A. *Methods of Dendrochronology: Applications in the Environmental Sciences*; Kluwer: Dordrecht, The Netherlands, 1990; pp. 104–122.
47. Cook, E.R.; Peters, K. Calculating unbiased tree-ring indices for the study of climatic and environmental change. *Holocene* **1997**, *7*, 361–370. [CrossRef]
48. Wigley, T.M.L.; Briffa, K.R.; Jones, P.D. On the average value of correlated times series, with applications in dendroclimatology and hydrometeorology. *J. Clim. Appl. Meteorol.* **1984**, *23*, 201–213. [CrossRef]
49. Harris, I.; Osborn, T.J.; Jones, P.; Lister, D. Version 4 of the CRU TS monthly high-resolution gridded multivariate climate dataset. *Sci. Data* **2020**, *7*, 109. [CrossRef] [PubMed]
50. Galakhov, V.P.; Mukhametov, R.M. *Glaciers of the Altai*; Nauka: Novosibirsk, Russia, 1999; 136p. (In Russian)
51. King, G.M.; Gugerli, F.; Fonti, P.; Frank, D. Tree growth response along an elevational gradient: Climate or genetics? *Oecologia* **2013**, *173*, 1587–1600. [CrossRef] [PubMed]
52. Moser, L.; Fonti, P.; Büntgen, U.; Esper, J.; Luterbacher, J.; Franzen, J.; Frank, D. Timing and duration of European larch growing season along altitudinal gradients in the Swiss Alps. *Tree Physiol.* **2010**, *30*, 225–233. [CrossRef]
53. Sugimoto, A.; Yanagisawa, N.; Naito, D.; Fujita, N.; Maximov, T.C. Importance of permafrost as a source of water for plants in east Siberian taiga. *Ecol. Res.* **2002**, *17*, 493–503. [CrossRef]
54. Vaganov, E.A.; Shiatov, S.G.; Mazepa, V.S. *Dendroclimatic Research in the Ural-Siberian Subarctic Zone*; Nauka: Novosibirsk, Russia, 1996; 246p. (In Russian)
55. Kirdyanov, A.V.; Prokushkin, A.S.; Tabakova, M.A. Tree-ring growth of Gmelin larch under contrasting local conditions in the north of Central Siberia. *Dendrochronologia* **2013**, *31*, 114–119. [CrossRef]
56. Kirdyanov, A.V.; Saurer, M.; Arzac, A.; Knorre, A.A.; Prokushkin, A.S.; Churakova, O.V.; Arosio, T.; Bebchuk, T.; Siegwolf, R.; Büntgen, U. Thawing permafrost can mitigate warming-induced drought stress in boreal forest trees. *Sci. Total Environ.* **2024**, *912*, 168858. [CrossRef]
57. Petrov, I.A.; Kharuk, V.I.; Golyukov, A.S.; Im, S.T.; Ondar, S.O.; Shushpanov, A.S. Siberian pine and larch response to warming-drying climate in the southern boundary of their range. *Forests* **2024**, *15*, 1054. [CrossRef]
58. Ovchinnikov, D.V.; Panjushkina, I.P.; Adamenko, M.F. The millennial tree-ring chronology of the Altai upland larch-tree and its use for the reconstruction of summer temperature. *Geogr. Nat. Resour.* **2002**, *1*, 102–108. (In Russian)
59. Taynik, A.V.; Barinov, V.V.; Oidupaa, O.C.; Myglan, V.S.; Reinig, F.; Büntgen, U. Growth coherency and climate sensitivity of *Larix sibirica* at the upper treeline in the Russian Altai-Sayan Mountains. *Dendrochronologia* **2016**, *39*, 10–16. [CrossRef]
60. Davi, N.K.; Rao, M.P.; Wilson, R.; Andreu-Hayles, L.; Oelkers, R.; D'Arrigo, R.; Nachin, B.; Buckley, B.; Pederson, N.; Leland, C.; et al. Accelerated recent warming and temperature variability over the past eight centuries in the Central Asian Altai from Blue Intensity in tree rings. *Geophys. Res. Lett.* **2021**, *48*, e2021GL092933. [CrossRef]
61. Park, W.K.; Telewski, F. Measuring maximum latewood density by image-analysis at the cellular level. *Wood Fiber Sci.* **1993**, *25*, 326–332.
62. Schweingruber, F.H.; Briffa, K.R.; Nogler, P. A tree-ring densitometric transect from Alaska to Labrador: Comparison of ring-width and maximum-latewood-density chronologies in the conifer belt of northern North America. *Int. J. Biometeorol.* **1993**, *37*, 151–169. [CrossRef]

63. Wilson, R.J.S.; Luckman, B.H. Dendroclimatic reconstruction of maximum summer temperatures from upper tree-line sites in interior British Columbia. *Holocene* **2003**, *13*, 853–863. [CrossRef]
64. Esper, J.; Krusic, P.; Ljungqvist, F.; Luterbacher, J.; Carrer, M.; Cook, E.; Davi, N.K.; Hartl-Meier, C.; Kirdyanov, A.; Konter, O.; et al. Ranking of tree-ring based temperature reconstructions of the past millennium. *Quat. Sci. Rev.* **2016**, *145*, 134–151. [CrossRef]
65. Björklund, J.; von Arx, G.; Nievergelt, D.; Wilson, R.; Van den Bulcke, J.; Günther, B.; Loader, N.J.; Rydval, M.; Fonti, P.; Scharnweber, T.; et al. Scientific Merits and Analytical Challenges of Tree-Ring Densitometry. *Rev. Geophys.* **2019**, *57*, 1224–1264. [CrossRef]
66. Björklund, J.; Seftigen, K.; Stoffel, M.; Fonti, M.V.; Kottlow, S.; Frank, D.C.; Esper, J.; Fonti, P.; Goosse, H.; Grudd, H.; et al. Fennoscandian tree-ring anatomy shows a warmer modern than medieval climate. *Nature* **2023**, *620*, 97–103. [CrossRef]
67. Silkin, P.P.; Kirdyanov, A.V.; Krusic, P.J.; Ekimov, M.V.; Barinov, V.V.; Büntgen, U. A new approach to measuring tree-ring density parameters. *J. Sib. Fed. Univ. Biol.* **2022**, *15*, 441–455.
68. Rydval, M.; Björklund, J.; von Arx, G.; Begović, K.; Lexa, M.; Nogueira, J.; Schurman, J.S.; Jiang, Y. Ultra-high-resolution reflected-light imaging for dendrochronology. *Dendrochronologia* **2024**, *83*, 126160. [CrossRef]
69. Schweingruber, F.H. *Tree Rings and Environment. Dendroecology*; Haupt: Berne, Switzerland, 1996; 609p.
70. Kirdyanov, A.V.; Vaganov, E.A.; Hughes, M.K. Separating the climatic signal from tree-ring width and maximum latewood density records. *Trees* **2007**, *21*, 37–44. [CrossRef]
71. Kramer, P.J.; Kozlowski, T.T. *Physiology of Woody Plants*; Academic Press: New York, NY, USA; San Francisco, CA, USA; London, UK, 1979; 811p.
72. Vaganov, E.A.; Hughes, M.K.; Shashkin, A.V. *Growth Dynamics of Conifer Tree Rings: Images of Past and Future Environments (Ecological Studies, Vol. 183)*; Springer Science & Business Media: Berlin, Germany, 2006; 356p.
73. Cook, E.R.; Esper, J.; D'Arrigo, R. Extra-tropical Northern Hemisphere land temperature variability over the past 1000 years. *Quat. Sci. Rev.* **2004**, *23*, 2063–2074. [CrossRef]
74. Kirdyanov, A.V.; Krusic, P.J.; Shishov, V.V.; Vaganov, E.A.; Fertikov, A.I.; Myglan, V.S.; Barinov, V.V.; Browse, J.; Esper, J.; Ilyin, V.A.; et al. Ecological and conceptual consequences of Arctic pollution. *Ecol. Lett.* **2020**, *23*, 1827–1837. [CrossRef]
75. Unkelbach, J.; Dulamsuren, C.; Behling, H. Late Holocene climate and land-use history in the Mongolian Altai Mountains: Combined evidence from palynological, macro-charcoal and tree-ring analyses. *Trees For. People* **2021**, *4*, 100073. [CrossRef]
76. Xiang, L.; Huang, X.; Sun, M.; Panizzo, V.N.; Huang, C.; Zheng, M.; Chen, X.; Chen, F. Prehistoric population expansion in Central Asia promoted by the Altai Holocene Climatic Optimum. *Nat. Commun.* **2023**, *14*, 3102. [CrossRef]